Review: Anharmonicity and necessity of phonon eigenvectors in the phonon normal mode analysis

Yuqing Huang (hyuqing@ncsu.edu)

Department of Nuclear Engineering, North Carolina State University, Raleigh, NC 27695-7909, USA.

Abstract

Molecular dynamics (MD) simulation are performed to study the impact of anharmonicity on eigenvectors of the dynamical matrix and the thermal conductivity calculations. Argon, silicon, germanium, silicon carbide and lead telluride are used as the test cases and the dynamical matrix is calculated by a Green's function based approach from Kong. Effects of anharmonicity on eigenvectors become significant only when there are at least two types of atoms basis in the primitive unit cell or multiple anharmonic interactions. Moreover, there are two formalizations of the frequency domain normal mode analysis (NMA) distinguished by the usage of eigenvectors. However, in the paper, it will be proved through both theoretical analysis and numerical analysis that these two forms are equivalent, and the eigenvectors are not required in the frequency domain NMA. Furthermore, typos for the equations in the paper, and the necessity of the eigenvectors will be discussed.

1. Introduction

With the discovery of the new materials and the improvement of the current materials, Thermal conductivity plays an essential role in studying these materials to improve energy transport in the materials. For example, carbon nanotubes, as nanostructured materials, have very high performance in the thermal properties. Thus the investigation of heat transport becomes more and more significant. Phonons are the dominant carriers for heat transfer in semiconductors and insulators when the conduction electron density is low [1]. Thus, studying phonon behavior is crucial in deeply understanding the thermal conductivity. Green Kubo method is an effective method to obtain thermal conductivity in a wide range of areas; however, it does not provide enough information about phonons. In order to capture the time evolution of the positions and velocities of phonons, the Boltzmann equation is introduced with a small number of phonons involving in a given collision [7]. In the Boltzmann framework, thermal conductivity can be expressed as $\boldsymbol{\kappa}_{therm} = \sum_{\boldsymbol{k}} \sum_{s} c_{ph} \boldsymbol{v}_g \boldsymbol{v}_g \tau$. Therefore, phonon dispersion relations and phonon lifetime τ are essential in computing thermal conductivity [2].

In the past few years, several analytical methods have been proposed and applied in calculating phonon relaxation time and thermal conductivity, such as quasi-harmonic lattice dynamic (LD) and anharmonic lattice dynamics (ALD). However, these models have their limitations due to different approximations. The quasi-harmonic LD method only captures thermal expansion, ignoring the effect directly from the anharmonicity [2]. ALD method only includes the third order of Taylor expansion for potential, thus it only valid in low temperature [2, 3]. Because of these limitations in the analytical models, numerical methods have developed based on the first principle method and molecular dynamics.

Molecular dynamics [4] is a suitable tool for analyzing the phonon properties since it includes the full anharmonicity of the atomic interaction. Zero-time correlation method [8], Kong's method [5, 6], Fourier

transform method [3], and a robust family of zero-time correlation method [9] are proposed and operated to calculate phonon dispersion relation, mode eigenvectors with full anharmonicity. These methods can extract information of phonons by projecting real-space trajectories on to normal mode coordinates or reciprocal space, which is the amplitude of the normal modes in a classical framework. This projection will involve the calculation of eigenvectors of the dynamical matrix. Normal mode analysis (NMA) in the time domain and the frequency domain are widely used in obtaining phonon lifetime and dispersion relation because of its simplicity and relatively low computational effort. There are two formalizations of frequency domain NMA. One needs eigenvectors, and another one does not. The detailed discussions will be introduced in the theory part. Several types of research have been done using different formalizations. For example, graphene [10, 23] and transition metal dichalcogenides [12] are studied by NMA analysis with eigenvectors obtaining from quasi-harmonic LD method while carbon nanotubes, PbTe [18] are using NMA analysis without eigenvectors. The latter one will have less computational cost. However, the equivalent of these two forms is still in discussion [1] [10]. Moreover, eigenvectors using in NMA analysis are obtained by quasi-harmonic LD calculation or LD calculations. Since a few of research considered anharmonicity effect on eigenvectors, it is not clear that using eigenvectors from LD calculation and ALD calculation will affect the result of thermal properties.

The purpose of this paper is to study the influence of anharmonicity on eigenvectors and settle the dispute in the necessity of eigenvectors in the NMA. The structure of this review is structured as follows. Firstly, we review the theoretical background of the methods. Secondly, a simple diatomic system with a different force constant will be analyzed. Thirdly, the anharmonicity effect on eigenvectors and the necessity of eigenvectors in NMA will be discussed. Finally, some comments and conclusions are provided.

2. Theory

2.1 Harmonic Oscillation

Under the harmonic approximation, the atoms vibrate with small amplitudes about their equilibrium positions. [7]. For the jth atom in the lth unit cell, the Taylor expansion of interatomic potential can be written in the form as Equation 1. N is the total number of atoms. For harmonic approximation, cubic term and higher-order terms will be neglected [7].

Equation 1

$$U = \frac{N}{2}\sum_{R\neq 0}\phi(R(j,l)) + \frac{1}{2}\sum_{R\neq R'}(u(jl) - u(j'l'))\cdot\nabla\phi(R(j,l) - R(j'l')) + \frac{1}{4}\sum_{R\neq R'}[(u(R(j,l)) - u(R(j'l'))\cdot\nabla]^2\phi(R(j,l) - R(j'l')) + O(u^3)$$

Based on the lattice dynamics theory, the frequencies and the eigenvectors for each mode can be obtained from solving the dynamic equation, as shown in Equation 2[7]. $\boldsymbol{e}(\boldsymbol{k}, s)$ is mode eigenvector matrix describing the relative atomic displacement, which can contain any arbitrary scale factor without changing the solution. Thus, it can be normalized, that is $(\boldsymbol{e}(k))^T(\boldsymbol{e}(k)) = 1$[8]. $\boldsymbol{D}(\boldsymbol{k})$ is $3N \times 3N$ dynamic matrix derived from the force constant matrix. Since force constant is the second derivative, it is easy to show that D(**k**) is Hermitian. The eigenvalues and eigenvectors of the dynamic matrix are corresponding to the square of frequencies and mode eigenvectors separately.

Equation 2

$$\boldsymbol{D}(\boldsymbol{k})\boldsymbol{e}(\boldsymbol{k},s) = \omega^2(\boldsymbol{k},s)\boldsymbol{e}(\boldsymbol{k},s)$$

2.2 Anharmonicity

In the real world, the system cannot be a rigid harmonic system; thus, anharmonicity of the system should be considered to describe thermal properties. With the anharmonicity, phonon can scatter from one state to another state, which leads to the finite thermal conductivity [7]. Also, as the temperature increase, it will have thermal expansion, which engenders the increasing distance between each other [8]. The increment in the distance will result in the reduction of the force exerted for each atom and frequency of normal modes [8].

Moreover, the anharmonic terms will include the higher-order terms in Taylor expansion, which can be shown in Equation 3 [7]. Usually, a cubic term or a quartic term will be considered. These extra terms in the potential will also influence the frequency with temperature.

Equation 3

$$U^{anh} = \sum_{n=3}^{\infty} \frac{1}{n!} \sum_{j_1 l_1 \cdots j_n l_n} D^n_{\mu_1 \cdots \mu_n}(j_1 l_1 \cdots j_n l_n) u_{\mu_1}(j_1 l_1) \cdots u_{\mu_n}(j_n l_n)$$
$$= \sum_{n=3}^{\infty} \frac{1}{n!} \sum_{\boldsymbol{k_1}, s_1} \sum_{\boldsymbol{k_2}, s_2} \cdots \sum_{\boldsymbol{k_n}, s_n} \boldsymbol{V}_n(k_1 s_1 \cdots \boldsymbol{k_n}, s_n)\, Q(\boldsymbol{k_1}, s_1) Q(\boldsymbol{k_2}, s_2) \ldots Q(\boldsymbol{k_n}, s_n) \Delta(\boldsymbol{k_1} + \boldsymbol{k_2} \ldots + \boldsymbol{k_n})$$

Where

$D^n_{\mu_1 \cdots \mu_n}(R_1 \cdots R_n) = \frac{\partial^n U}{\partial \mu_1(R_1) \cdots \partial \mu_n(R_n)}|_{u=0}$ and $\boldsymbol{V}_n(k_1 s_1 \cdots \boldsymbol{k_n}, s_n) = \sum_{j_1 j_2 l_2' \ldots j_n l_n'} D^n_{\mu_1 \cdots \mu_n}(j_1 0 \cdots j_n' l_n') exp(\boldsymbol{k_2} \cdot (\boldsymbol{r}(j_2 l_2') - \boldsymbol{r}(j_1 0))) \ldots exp(\boldsymbol{k_n} \cdot (\boldsymbol{r}(j_n l_n') - \boldsymbol{r}(j_1 0)))$

2.3 NMA methods

For the small perturbation, normal mode amplitudes can be written as the perturbation form with frequency shift Δ and linewidth $\Gamma_{k,}$ as Equation 5, since the anharmonic terms will make the phonon spectrum to broaden and shift [14]. Based on this equation and definition for phonon relaxation time, the lifetime and linewidth are related by $\tau_{k,s} = (2\Gamma_{k,s})^{-1}$. The shortcoming for the NMA methods is that it cannot detect the individual phonon and phonon scattering, and thus the normal process and Umklapp process cannot be distinguished [25]. The normal process will not contribute to the thermal resistive, and the finite thermal conductivity is mainly contributed by the Umklapp process [7].

Equation 4

$$Q(\boldsymbol{k}, s, t) = Q_{k,s,0} exp(i(\omega_{k,s} + \Delta + i\Gamma_{k,s}))$$

2.3.1 Normal mode analysis in the time domain

Normal mode analysis in the time domain is firstly proposed by Ladd, A., et al. [14]. From MD simulation, velocities and positions for each atom can be recorded for each time step. The obtained velocities and

calculated displacements will be projected on the normal mode coordination as Equation 5. The mode eigenvectors can be obtained from quasi-harmonic LD calculations.

Equation 5

$$Q(\boldsymbol{k},s,t)=\frac{1}{\sqrt{N_u}}\sum_{j,\mu}\sum_{l}\sqrt{m_j}e^{*}_{j,\mu}(\boldsymbol{k},s)\exp\left(-i(\boldsymbol{k}\cdot\boldsymbol{r_l})\right)u_\mu(\mathrm{j,l,t})=\sum_{j,\mu}e^{*}_{j,\mu}(\boldsymbol{k},s)q_{j,\mu}(\mathrm{k,t})$$

Since the ensemble-averaged heat current is zero and the number of phonons will be proportional to the energy [14], the correlation of the total energy can be fitted by exponential decay form [14-16]. $\tau_{k,\upsilon}$ is phonon relaxation time for one mode which can be extracted from Equation 6

Equation 6

$$\frac{<E_{k,\mu}(t)E_{k,\mu}(0)>}{<E_{k,\mu}(0)E_{k,\mu}(0)>}=e^{-\frac{t}{\tau_{k,\upsilon}}}$$

$$E_{k,\mu}(t)=KE+PE\ =\frac{1}{2}|\dot{Q}(\boldsymbol{k},s)|^2+\frac{1}{2}{\omega_s}^2(k)|Q(k,s)|^2$$

2.3.2 Normal mode analysis in the frequency domain

In the frequency domain, normal mode analysis has two different forms. One is calculating the total spectral energy density (SED), and another is calculating the total spectral kinetic energy density. The average kinetic energy can be computed from Equation 7[17].

Equation 7

$$T(k,s,t)=\frac{1}{2}\lim_{\tau_0\to\infty}\frac{1}{\tau_0}\int_0^{\tau_0}\dot{Q}*(\boldsymbol{k},s,t)\dot{Q}(\boldsymbol{k},s,t)\,dt$$

The spectral energy density can be obtained by transforming kinetic energy from the time domain to the frequency domain through Parseval's theorem [17].

$$T(k,s,\omega)=\lim_{\tau_0\to\infty}\frac{1}{4\pi\tau_0}\sum_{\boldsymbol{j},\mu}|\int_0^{\tau_0}\dot{Q}(\boldsymbol{k},s,t)exp(-i\omega t)\,dt|^2$$

In the equation, factor 2 is from the equipartition that average kinetic energy will be equal to the average potential energy [20]. The total spectral energy density is calculated by summing over all the SED of each branch, which is a superposition of 3n Lorentzian function with center $\omega^A_{k,s}$ and width $\Gamma_{k,s}$ (full derivation in the reference [13]).

$$\Phi(k,\omega)=2\sum_s T(k,s,\omega)=\sum_s\lim_{\tau_0\to\infty}\frac{1}{2\pi\tau_0}\sum_{\boldsymbol{j},\mu}|\int_0^{\tau_0}\dot{Q}(\boldsymbol{k},s,t)exp(-i\omega t)\,dt|^2=\sum_s\frac{C_{k,s}}{(\omega-\omega^A_{k,s})^2+\Gamma^2_{k,s}}$$

$C_{k,s}=q^2_{k,s,0}({\omega^A_{k,s}}^2+\Gamma^2_{k,s})$ is constant related to wavevectors k and mode labels s. Phonon relaxation time can be extracted by fitting the SED by 3n Lorentzian function for each branch.

Another form is by putting the derivative of the normal mode coordinates into summing over kinetic spectral density $T(k,s,\omega)$ of each branch.

$$\Phi'(k,\omega)$$
$$= \sum_s \lim_{\tau_0\to\infty} \frac{1}{4\pi\tau_0 N_u} \sum_{\boldsymbol{j},\mu} |\int_0^{\tau_0} \sum_l \sqrt{m_j} e^*_{j,\mu}(\boldsymbol{k},s) \exp\left(-i(\boldsymbol{k}\cdot\boldsymbol{r_l})\right) \dot{u}_\mu(\mathrm{j,l,t})\, exp(-i\omega t)\, dt|^2$$
$$= \lim_{\tau_0\to\infty} \frac{1}{4\pi\tau_0 N_u} \sum_{\boldsymbol{j},\mu} m_j [|\int_0^{\tau_0} \sum_l \exp\left(-i(\boldsymbol{k}\boldsymbol{r_l})\right) \dot{u}_\mu(\mathrm{j,l,t})\, exp(-i\omega t)\, dt|^2 \,|\sum_s e^*_{j,\mu}(\boldsymbol{k},s)\,|^2]$$
$$= \lim_{\tau_0\to\infty} \frac{1}{4\pi\tau_0 N_u} \sum_{\boldsymbol{j},\mu} m_j |\int_0^{\tau_0} \sum_{j,\mu} \sum_l \exp\left(-i(\boldsymbol{k}\cdot\boldsymbol{r_l})\right) \dot{u}_\mu(\mathrm{j,l,t})\, exp(-i\omega t)\, dt|^2$$

Because of eigenvectors are orthonormal and normalized, $\sum_s e^*_{j,\mu}(\boldsymbol{k},s) e_{j,\mu}(\boldsymbol{k},s) = 1$. Thus, for the second expression, the eigenvectors are not needed. The phonon relaxation time can be extracted by fitting SED by the superposition of the 3n Lorentzian function.

2.4 Green's Function based approach from Kong

Kong's method is based on the equipartition theorem and Green's function to approximate the phonon dispersion. The dynamics matrix can be obtained from

Equation *8* [5, 6]. The displacement of atoms can be directly calculated from MD simulation and project them into reciprocal space. The denominator in the equation is evaluated by projecting the displacement in the reciprocal space and doing the ensemble average. The frequency can be directly extracted from calculating the eigenvalues and eigenvector of dynamics matrices [5, 6].

Equation 8

$$D_{j\mu j'\upsilon}(\boldsymbol{q}) = \frac{k_b T}{< \widetilde{u_{j\mu}}(\boldsymbol{q}) \widetilde{u_{j'\upsilon}} * (\boldsymbol{q}) >}$$

$where\ \tilde{u}(\boldsymbol{q},\boldsymbol{t}) = \frac{1}{\sqrt{N_u}} \sum_l \sqrt{m_j} u_\mu(j,l,t) exp(-i\boldsymbol{q}r_l) = \frac{1}{\sqrt{N_u}} (\sum_l \sqrt{m_j} r_\mu(j,l,t) exp(-i\boldsymbol{q}r_l) - \sum_l \sqrt{m_j}\bar{r_\mu}(j,l,t) exp(-i\boldsymbol{q}r_l)$

3. Harmonic approximation analysis for diatomic chain [16]

The diatomic chain is composed of two atoms: atoms A with mass m_1 and atoms B with mass m_2 and the spring constants are Γ_2 and Γ_1, as shown in Figure 1. The Newton motion equation can be easily written as Equation 9, and the frequency can be obtained by solving the characteristic equation for ω. The frequency is obtained as in Equation 10. There are two different frequency for given wavevectors. The positive sign and the negative sign are corresponding to the optical modes and acoustic modes separately. For optical modes, two atoms in a unit cell will move in the opposite direction, and for acoustic modes, they will move in the same direction along the wavevector. The amplitudes of the mode eigenvectors can represent the relative amplitudes of the movement for each atom in the unit cell.

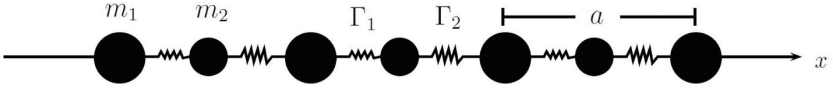

Figure 1 diatomic chain

Equation 9

$$m_1\ddot{u}_1(na) = -\frac{\partial U^{harm}}{\partial u_1(na)} = -\Gamma_1[u_1(na) - u_2(na)] - \Gamma_2[u_1(na) - u_2([n-1]a)]$$

$$m_2\ddot{u}_2(na) = -\frac{\partial U^{harm}}{\partial u_2(na)} = -\Gamma_1[u_2(na) - u_1(na)] - \Gamma_2[u_2(na) - u_1([n+1]a)]$$

Equation 10

$$\omega_{\pm}{}^2 = \frac{1}{2m_1m_2}[(m_1+m_2)(\Gamma_2+\Gamma_1) \pm \sqrt{(m_1+m_2)^2(\Gamma_2+\Gamma_1)^2 - 8\Gamma_1\Gamma_2\big(1-cos(ka)\big)m_1m_2}]$$

Since eigenvector is normalized, $(\boldsymbol{e}(\boldsymbol{k}))^*(\boldsymbol{e}(\boldsymbol{k}))$ is equal to one. Thus, one can use the ratio of magnitude eigenvectors to determine whether eigenvectors are changed. The ratio of the magnitude of the eigenvectors for acoustic modes is shown in Equation 11. If the ratio of the mass $\eta = 1$, which means that two basis atoms are the same, then $\frac{|e_2(k,s)|}{|e_1(k,s)|} = 1$. Thus, eigenvectors will not change as the variance of force constant with temperature. Also, for the k in the limit of 0, the $\frac{|e_2(k,s)|}{|e_1(k,s)|}$ will not depend on force constants. Optical modes can do the same analysis. The ratio of the eigenvectors will be the inverse of that for the acoustic modes, which represents in Appendix B.

Equation 11

$$\frac{|e_2(k,s)|}{|e_1(k,s)|} = \frac{(1-\eta)(\xi+1) + \sqrt{(\eta+1)^2(1+\xi)^2 - 16\xi sin^2(\frac{ka}{2})\eta}}{2\sqrt{(1+\xi)^2 - 2\xi\big(1-cos(ka)\big)}}$$

Since mathematically, the effect of the anharmonicity on atoms can be viewed as the change of force constant. Thus, the author purposed two requirements that the eigenvectors will be affected by anharmonicity involved or get stronger. The first one is that the system contains at least two types of basis atoms in the primitive unit cell, and the second one is that each atom has different anharmonic interactions with other atoms.

4. Simulation details [16]

In order to test the requirements of anharmonicity effect on eigenvectors, three groups of the materials are used: (1) only one type of the basis atom in primitive unit cell: Argon, diamond, silicon, germanium. (2) two types of basis atom but it has the same anharmonic interaction: β - SiC. (3) two types basis and different anharmonic interactions: PbTe. The LD calculation is conducted in 0K with GULP, and MD simulation using a Green's function-based approach from Kong is conducted in 20 K and 800 K to obtain the eigenvectors. MD simulation is conducted in LAMMPS. $8 \times 8 \times 8$ unit cells will be used (that is, 2048 atoms for Ar and 4096 atoms for C, Si, Ge, SiC, and PbTe). The frequency and eigenvector are calculated for 9 points of wavevector in the [1, 0, 0] direction. Since argon is rare gas, the interaction potential used for the rare gas is Lennard-Jones (LJ) potential. Diamond, Si, Ge, and β - SiC, as a covalent crystal, used Tersoff potential, which describes the strength of each bond with bond order [21]. Buckingham potential has been used for PbTe crystal. The parameters chosen for the potentials of SiC and PbTe are attached at appendix A. For β - SiC, only nearest neighbors of atoms are considered while for PbTe, both the nearest

neighbors and longer-range interactions will be considered. In the Gramma points, 20 iteration steps are used to enforce the acoustic sum rule. Also, MD simulations will be performed in 300 K for bulk argon, silicon, germanium and PbTe to obtained SED.

5. Result and analysis [16]

Argon, diamond, silicon, germanium only have one type of basis atom in the primitive unit cell. The eigenvectors from LD calculation and MD simulation are the same and constant. It can also be obtained by theoretical analysis qualitatively. One can take argon as an example and only consider longitudinal acoustic modes. The nearest neighbors for a single argon atom in the single plane are $\frac{a}{2}[1,\pm1,0]$ and $\frac{a}{2}[1,0,\pm1]$. Thus, the effective force constant is shown in Equation 12. Γ is the second derivative of potential. It will change with temperature as the atomic structures change and anharmonicity becomes stronger. Now, the system can be considered as diatomic chains. Since there is only one type of atom in the primitive cell, it can be considered that two atoms with the same mass are in the larger cell and the same anharmonic interactions. From Equation 11, the ratio of the magnitude of eigenvectors does not depend on the effective force constant, and it will be equal to 1. Thus, for one basis atoms in the primitive unit cell, $\boldsymbol{e} = (e, 0,0)$ with |e| =1 and for other three crystals with two same basis atoms in the primitive unit cell, $\boldsymbol{e} = (e_1, 0,0; e_2, 0,0)$ with $|e_1| = |e_2| = \frac{1}{\sqrt{2}}$.

Equation 12

$$K_{eff} = \frac{\partial^2 U}{\partial x^2} = \frac{\partial^2 U}{\partial r^2}(\frac{x}{r})^2 = 2\frac{\partial^2 U}{\partial r^2} = 2\Gamma$$

The result for β - SiC shows that it is the same for the eigenvectors at different temperatures. However, the author does not show the result. The same analysis can also be conducted for β - SiC. The effective force constant will be the same for Si and C. From Equation 11, since the ratio of force constants is constant, the anharmonicity will not affect the eigenvectors for this type of the materials, but it will not be different with wavevectors.

For PbTe, it meets all the requirements for existing anharmonic eigenvectors. It has different types of atom basis and interactions. The ratio of the magnitude of the eigenvector with three different temperatures is shown in Figure 2. Since the eigenvectors represent the contribution of each basis atom to the amplitudes of movement, the large $|e_{Pb}|$ in acoustic mode represents that the vibration modes of the Pb are dominated in the longitudinal acoustic mode, which is mainly due to the effect that heavier Pb atoms will generally produce lower frequencies [18]. For the lower temperature 20K, the anharmonicity effect on the eigenvectors is not apparent. However, for the higher temperature 800K, this effect will be pronounced specially for the midpoint wavevector, which can reach a 50% difference. When k is close to zero, the eigenvectors are not sensitive to the anharmonicity, and it is close to the square root of the mass ratio. The contributing factor might be long-wavelength normal modes. When the wavelength is larger than the spacing between the atoms, crystal can seem like a continuous and the small changes in structure will not be observed by the long-wavelength waves.

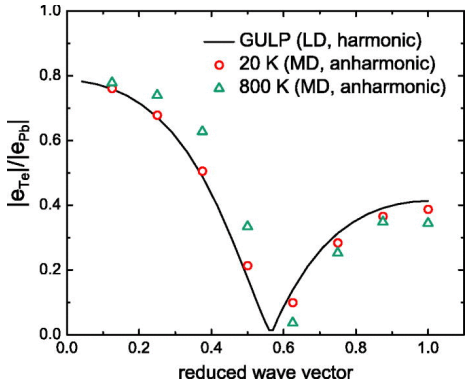

Figure 2 The ratio $|e_{Te}|/|e_{Pb}|$ as a function of reduced wave vector in the [1, 0, 0] direction for the LA mode of bulk PbTe at different temperatures, where $|e_{Te}|$ and $|e_{Pb}|$ are the moduli of the components of the eigenvector (e_{Pb},0,0;e_{Te},0,0). The x axis for the reduce wave vector is obtained from $k^* = \frac{k}{2\pi/a}$ (from [16])

From the theory part of NMA in the time domain and frequency domain, eigenvectors are needed for the time domain NMA and first formalization of the frequency domain NMA. However, it is not necessary for the second form of the frequency domain NMA. Nevertheless, these two forms of the frequency domain will give the same result. In order to demonstrate this statement, $\dot{Q}(k,s,\omega)$ can be written in vector format, as shown in Equation 13.

$$\Phi(k,\omega) = \sum_s |\dot{Q}(k,s,\omega)|^2$$

Equation 13

$$\begin{aligned}|\dot{Q}(k,s,\omega)|^2 &= |\boldsymbol{e}^\dagger(k,s)\dot{\boldsymbol{q}}(k,\omega)|^2 = (\boldsymbol{e}^\dagger(k,s)\dot{\boldsymbol{q}}(k,\omega))^\dagger((\boldsymbol{e}^\dagger(k,s)\dot{\boldsymbol{q}}(k,\omega)) \\ &= \dot{\boldsymbol{q}}(k,\omega)^\dagger \boldsymbol{e}(k,s)\boldsymbol{e}^\dagger(k,s)\dot{\boldsymbol{q}}(k,\omega)\end{aligned}$$

$\dot{\boldsymbol{q}}(k,\omega)$ and $\boldsymbol{e}(k,s)$ is the $1 \times N$ matrix containing the eigenvector for each atom in each direction. The summing over all the SED for each branch is shown:

$$\begin{aligned}\Phi(k,\omega) &= \sum_s \dot{\boldsymbol{q}}(k,\omega)^\dagger \boldsymbol{e}(k,s)\boldsymbol{e}^\dagger(k,s)\dot{\boldsymbol{q}}(k,\omega) = \dot{\boldsymbol{q}}(k,\omega)^\dagger \sum_s \boldsymbol{e}(k,s)\boldsymbol{e}^\dagger(k,s)\,\dot{\boldsymbol{q}}(k,\omega) \\ &= \dot{\boldsymbol{q}}(k,\omega)^\dagger \mathbf{I}\dot{\boldsymbol{q}}(k,\omega) = \dot{\boldsymbol{q}}(k,\omega)^\dagger \dot{\boldsymbol{q}}(k,\omega) = \Phi'(k,\omega)\end{aligned}$$

From here, two forms of frequency domain SEDs are completely equivalent. Therefore, total SEDs will not be related to eigenvectors if they are orthonormal. MD simulations have been conducted to obtain SEDs with true eigenvectors and any arbitrary orthonormal eigenvectors for argon, silicon, germanium, and lead telluride in 300K. The results show that total SEDs are exactly the same with different orthonormal eigenvectors. The result for PbTe at reduced wavevector $(0.875, 0, 0)$ is shown in Figure 3. From the figure, it can be observed that although SED for each branch is different, SEDs for summing over all these branches in certain wavevector are the same. Thus, eigenvectors in the frequency domain NMA are not necessary.

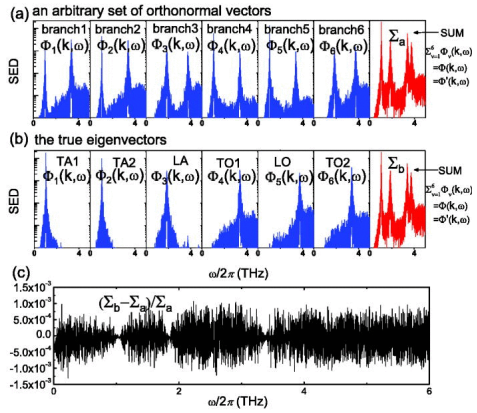

Figure 3 The SED functions of bulk PbTe calculated based on (a) an arbitrary set of orthonormal vectors and (b) the true eigenvectors at the temperature of 300 K and the reduced wave vector of (0.875, 0, 0). Figure (c) shows the relative difference between the total SEDs given by (a) and (b) (from [16])

6. Comments

After reviewing this paper, there are several comments about the importance and improvements to it.

6.1 Importance of the paper

This paper solved the previous debate in two formalizations for SEDs in frequency domain NMA. Jason M. Larkin et al. in 2012 compared the spectral energy density, phonon relaxation, and thermal conductivity for Argon and Silicon. From their studies, Φ' does not equal to Φ, but the major features are the same, and the difference between Φ' and Φ will reduce with the increment of temperature. Also, phonon lifetime is different regardless of low frequency and high frequency, thus they claimed that without using eigenvector will cause some vital factors missing in Φ'. However, this paper based on mathematical analysis and numerical analysis to prove that although there is a constant factor difference between Φ' and Φ, the total SED provides the same information for phonon lifetime. Thus, the main reason that will affect the correctness of phonon lifetime in Φ' might depend on the resolution of SED, although the decrease in discrepancy and the overestimate of phonon lifetime should be continued to study. As the temperature increases, anharmonicity will become stronger and thus broaden the linewidth of SEDs because of more scattering involved. This broadening will cause that some peaks cannot be distinguished between others and thus underestimates phonon lifetime. For degeneracy branches, it has the same problem for the method without eigenvectors. Thus, the principal purpose of eigenvectors in the frequency domain NMA is to avoid the errors yielded by undistinguishing broadened spectral density for each branch. Also, it will offer the rational basis that using LD and quasi-harmonic LD to obtain the eigenvector in frequency domain will not generate errors for materials with multiple basis atoms and anharmonic interactions, which can reduce the computational effort.

In addition, the influence of anharmonicity in the eigenvectors has been proved for the materials with multiple basis atoms and anharmonic interactions. In the time domain NMA, the eigenvector is required to transform the position and velocity onto the normal coordinates. Also, eigenvectors are necessary for many other areas such as calculating instantaneous heat current [25] and individual phonon scattering [24]. Therefore, the materials that do not meet the requirements, LD calculation can be used to obtain the

eigenvectors, which can reduce the computational cost compared to calculation with full anharmonicity. For materials like PbTe, PbSe, and Bi_2Te_3, the anharmonic eigenvectors will become important.

6.2 Improvements

6.2.1 Typos in the equation

In the paper, the magnitude of the ratio of the eigenvector has a little typo. For diatomic mode, this ratio should be as Equation 14.

Equation 14

$$\frac{|e_2(k,s)|}{|e_1(k,s)|} = \frac{(1-\eta)(\xi+1)+\sqrt{(\eta+1)^2(1+\xi)^2-8\eta\xi(1-cos(ka))}}{2\sqrt{\eta}\sqrt{(1+\xi)^2-2\xi\big(1-cos(ka)\big)}}$$

The full deviation is shown in appendix B. It can also be approved from Figure 2. When k is in the limit of 0, $\frac{|e_2(k,s)|}{|e_1(k,s)|} = \frac{1}{\sqrt{\eta}}$ from Equation 14. However, from Equation 11, $\frac{|e_2(k,s)|}{|e_1(k,s)|} = 1$. From Figure 2, when k is close to 0, $\frac{|e_2(k,s)|}{|e_1(k,s)|} = \sqrt{\frac{M_{Te}}{M_{Pb}}} = \sqrt{\frac{127.6u}{207.2u}} = 0.7847$. This square root of mass-ratio is from the displacement weighted by square root of the atomic mass.

For the proof of the equivalent of two forms in frequency domain NMA, $\Phi(k,\omega)$ should be equal to $2\Phi'(k,\omega)$. This factor of 2 is from the definition of these two forms. Thus, SED for these two forms has different intensity, but it will provide the same information for phonon lifetime and frequency. The additional two in the equation can explain why in the result from Jason M. Larkin's work [1][13] that there is a gap between the SEDs for Argon obtaining from these two formalizations only in the intensity and center and width of them is same.

6.2.2 Force field

The correctness of results from the simulation will mainly depend on the force field. The method describes above, including Kong's method and NMA method will involve the velocities and displacements from MD simulation. The realistic of these parameters depends on the interactions between each atom. For example, the dispersion curve obtained from Porter, L. J., et al. is not agreed well with the experimental results especially in optical branches, since β - Si is known to be 12% ionic crystal whereas Tersoff potential only describes covalent bonding [19]. Finding a model that can describe the interaction between the atoms to reach the accuracy comparable to the first principle method and the computational cost comparable to MD simulation is still a challenge.

7. Conclusion

For compound materials with different interactions, anharmonicity effect on eigenvectors will become more critical as temperature increases. Moreover, this paper resolved the contention about the role of the eigenvector in NMA in previous years. Eigenvectors are necessary for the time domain NMA; thus, eigenvectors obtained from full anharmonicity may improve the accuracy of predicting the thermal properties for the materials that meet the two requirements. However, for the frequency domain NMA, since the total SEDs do not require the eigenvectors, anharmonic eigenvectors may not be useful, and it is

suitable for using eigenvector from LD calculation or quasi-harmonic LD calculation to distinguish the SEDs for each branch.

Although there are still many studies that should be done in calculating thermal conductivity such as force field in MD simulation, and finite-size effect broadening phonon spectrum, the work of this paper is an excellent study for solving the two critical problems.

Reference

[1] Larkin, J., et al. (2014). "Comparison and Evaluation of Spectral Energy Methods for Predicting Phonon Properties." Journal of Computational and Theoretical Nanoscience 11: 249-256.

[2] Turney, J. E., et al. (2009). "Predicting phonon properties and thermal conductivity from anharmonic lattice dynamics calculations and molecular dynamics simulations." Physical Review B 79(6): 064301.

[3] Wang, C. Z., et al. (1989). "Molecular-dynamics study of anharmonic effects in silicon." Physical Review B 40(5): 3390-3393.

[4] McGaughey, A. J. H. and J. M. J. A. R. o. H. T. Larkin (2014). "Predicting phonon properties from equilibrium molecular dynamics simulations." Annual Review of Heat Transfer, 17: 49-87.

[5] Kong, L. T., et al. (2009). "Implementation of Green's function molecular dynamics: An extension to LAMMPS." Computer Physics Communications 180(6): 1004-1010.

[6] Kong, L. T. (2011). "Phonon dispersion measured directly from molecular dynamics simulations." Computer Physics Communications 182(10): 2201-2207.

[7] Ashcroft, N. W. and N. D. Mermin (1976). Solid state physics. Philadelphia, Saunders College.

[8] Dove, M. T. (1993). Introduction to Lattice Dynamics. Cambridge, Cambridge University Press.

[9] Raj, A. and J. Eapen (2019). "Phonon dispersion using the ratio of zero-time correlations among conjugate variables: Computing full phonon dispersion surface of graphene." Computer Physics Communications 238: 124-137.

[10] Qiu, B. and X. Ruan (2012). "Reduction of spectral phonon relaxation times from suspended to supported graphene." Applied Physics Letters 100(19): 193101.

[11] Qiu, B., et al. (2012). "Molecular dynamics simulations of lattice thermal conductivity and spectral phonon mean free path of PbTe: Bulk and nanostructures." Computational Materials Science 53(1): 278-285.

[12] Mobaraki, A., et al. (2019). "Temperature-dependent phonon spectrum of transition metal dichalcogenides calculated from the spectral energy density: Lattice thermal conductivity as an application." Physical Review B 100(3): 035402.

[13] Larkin, Jason M., Massicotte, Alexandre D., Turney, Joseph E., McGaughey, Alan J. H., and Amon, Cristina H. "Comparison of Spectral Energy Density Methods for Predicting Phonon Properties." Proceedings of the ASME 2012 Third International Conference on Micro/Nanoscale Heat and Mass Transfer. ASME 2012 Third International Conference on Micro/Nanoscale Heat and Mass Transfer. Atlanta, Georgia, USA. March 3–6, 2012. pp. 753-759. ASME.

[14] Ladd, A., et al. (1986). "Lattice thermal conductivity: A comparison of molecular dynamics and anharmonic lattice dynamics." Physical review. B, Condensed matter 34: 5058-5064.

[15] Feng, T. and X. Ruan (2014). "Prediction of Spectral Phonon Mean Free Path and Thermal Conductivity with Applications to Thermoelectrics and Thermal Management: A Review." Journal of Nanomaterials 2014: 206370.

[16] Feng, T., et al. (2015). "Anharmonicity and necessity of phonon eigenvectors in the phonon normal mode analysis." 117(19): 195102.

[17] Thomas, J. A., et al. (2010). "Predicting phonon dispersion relations and lifetimes from the spectral energy density." Physical Review B 81(8): 081411.

[18] Qiu, B., et al. (2012). "Molecular dynamics simulations of lattice thermal conductivity and spectral phonon mean free path of PbTe: Bulk and nanostructures." Computational Materials Science 53(1): 278-285.

[19] Porter, L. J., et al. (1997). "Atomistic modeling of finite-temperature properties of β-SiC. I. Lattice vibrations, heat capacity, and thermal expansion." Journal of Nuclear Materials 246(1): 53-59.

[20] Huang, K. (1987). Statistical Mechanics, Wiley.

[21] Tersoff, J. (1988). "New empirical approach for the structure and energy of covalent systems." Physical Review B 37(12): 6991-7000.

[22] Rapaport, D.C, “The art of molecular dynamics simulation”, Cambridge University Press, New York (2004).

[23] Zou, J.-H., et al. (2016). "Phonon thermal properties of graphene from molecular dynamics using different potentials." 145(13): 134705.

[24] Raj, A. and J. Eapen (2019). "Deducing Phonon Scattering from Normal Mode Excitations." Scientific Reports 9(1): 7982.

[25] Raj, A. and J. Eapen (2019). "Exact diagonal representation of normal mode energy, occupation number, and heat current for phonon-dominated thermal transport." The Journal of Chemical Physics 151(10): 104110.

Appendix A

Table 1 Parameters used in the interatomic potential for PbTe and partially charged used to account for electrostatics: Pb: +0.666, Te: -0.666

	A(eV)	ρ(Å)	$C(eV\ Å^6)$	Range(Å)
Pb-Pb	84203.2	0.0754	61.01	16.0
Pb-Te	92131.5	0.2552	585.70	16.0
Te-Te	1773611.7	0.2565	0.61	16.0

Table 2 the parameters for Tersoff potential [7]

Parameters	Carbon	Silicon
A(eV)	1.5448×10^3	1.8308×10^3
B(eV)	3.8963×10^2	4.7118×10^2
$\lambda(nm^{-1})$	0.34653	0.24799
$\mu(nm^{-1})$	0.23064	0.17322
β	4.1612×10^{-6}	1.1000×10^{-6}
n	0.99054	0.78734
c	1.9981×10^4	1.0039×10^5
d	7.0340	16.217
h	-0.39953	-0.59825
R(nm)	0.25	0.25
S(nm)	0.21	0.30
$\chi_{Si-C} = 1.0086$		

Appendix B

$$U^{harm} = \frac{\Gamma_1}{2}\sum_n [u_1(na) - u_2(na)]^2 + \frac{\Gamma_2}{2}\sum_n [u_1(na) - u_2([n+1]a)]^2 \qquad (B-1)$$

$$m_1\ddot{u}_1(na) = -\frac{\partial U^{harm}}{\partial u_1(na)} = -\Gamma_1[u_1(na) - u_2(na)] - \Gamma_2[u_1(na) - u_2([n-1]a)] \qquad (B-2)$$

$$m_2\ddot{u}_2(na) = -\frac{\partial U^{harm}}{\partial u_2(na)} = -\Gamma_1[u_2(na) - u_1(na)] - \Gamma_2[u_2(na) - u_1([n+1]a)] \qquad (B-3)$$

$$u_1(na) = \frac{1}{\sqrt{m_1}}A(k,s,t)e_1(k,s)exp\big(i(kna - \omega t)\big) \qquad (B-4)$$

$$u_2(na) = \frac{1}{\sqrt{m_2}}A(k,s,t)e_2(k,s)exp\big(i(kna - \omega t)\big) \qquad (B-5)$$

$$-m_1\omega^2\frac{1}{\sqrt{m_1}}A(k,s,t)e_1(k,s) = -\Gamma_1\left[\frac{1}{\sqrt{m_1}}A(k,s,t)e_1(k,s) - \frac{1}{\sqrt{m_2}}A(k,s,t)e_2(k,s)\right] - \Gamma_2\left[\frac{1}{\sqrt{m_1}}A(k,s,t)e_1(k,s) - \frac{1}{\sqrt{m_2}}A(k,s,t)e_2(k,s)exp(i(-ka))\right] \qquad (B-6)$$

$$-m_2\omega^2\frac{1}{\sqrt{m_2}}A(k,s,t)e_2(k,s) = -\Gamma_1\left[\frac{1}{\sqrt{m_2}}A(k,s,t)e_2(k,s) - \frac{1}{\sqrt{m_1}}A(k,s,t)e_1(k,s)\right] - \Gamma_2\left[\frac{1}{\sqrt{m_2}}A(k,s,t)e_2(k,s) - \frac{1}{\sqrt{m_1}}A(k,s,t)e_1(k,s)exp(i(ka))\right] \qquad (B-7)$$

$$\omega^2\begin{bmatrix}e_1(k,s)\\ e_2(k,s)\end{bmatrix} = \begin{bmatrix}\frac{\Gamma_2+\Gamma_1}{m_1} & -\frac{1}{\sqrt{m_1}\sqrt{m_2}}\big(\Gamma_1 + \Gamma_2 exp(-ika)\big)\\ -\frac{1}{\sqrt{m_1}\sqrt{m_2}}\big(\Gamma_1 + \Gamma_2 exp(ika)\big) & \frac{\Gamma_2+\Gamma_1}{m_2}\end{bmatrix}\begin{bmatrix}e_1(k,s)\\ e_2(k,s)\end{bmatrix} \qquad (B-8)$$

$$\begin{bmatrix}\omega^2 - \frac{\Gamma_2+\Gamma_1}{m_1} & \frac{1}{\sqrt{m_1}\sqrt{m_2}}(\Gamma_1 + \Gamma_2 exp(-ika)\\ \frac{1}{\sqrt{m_1}\sqrt{m_2}}\big(\Gamma_1 + \Gamma_2 exp(ika)\big) & \omega^2 - \frac{\Gamma_2+\Gamma_1}{m_2}\end{bmatrix}\begin{bmatrix}e_1(k,s)\\ e_2(k,s)\end{bmatrix} = 0 \qquad (B-9)$$

$$det\begin{vmatrix}\omega^2 - \frac{\Gamma_2+\Gamma_1}{m_1} & \frac{1}{\sqrt{m_1}\sqrt{m_2}}\big(\Gamma_1 + \Gamma_2 exp(-ika)\big)\\ \frac{1}{\sqrt{m_1}\sqrt{m_2}}\big(\Gamma_1 + \Gamma_2 exp(ika)\big) & \omega^2 - \frac{\Gamma_2+\Gamma_1}{m_2}\end{vmatrix} = 0 \qquad (B-10)$$

$$\omega^4 - (\frac{m_1+m_2}{m_1m_2}(\Gamma_2+\Gamma_1))\omega^2 + \frac{2\Gamma_1\Gamma_2(1-cos(ka))}{m_1m_2} = 0 \qquad (B-11)$$

$$\omega_{\pm}{}^2 = \frac{1}{2}(\frac{m_1+m_2}{m_1m_2}(\Gamma_2+\Gamma_1) \pm \sqrt{(\frac{m_1+m_2}{m_1m_2}(\Gamma_2+\Gamma_1))^2 + 4\frac{2\Gamma_1\Gamma_2(1-cos(ka))}{m_1m_2}}$$

$$= \frac{1}{2m_1m_2}[(m_1+m_2)(\Gamma_2+\Gamma_1) \pm \sqrt{(m_1+m_2)^2(\Gamma_2+\Gamma_1)^2 - 8\Gamma_1\Gamma_2(1-cos(ka))m_1m_2}]$$

$$= \frac{1}{2m_1m_2}[(m_1+m_2)(\Gamma_2+\Gamma_1) \pm \sqrt{(m_1+m_2)^2(\Gamma_2+\Gamma_1)^2 - 16\Gamma_1\Gamma_2 sin^2(\frac{ka}{2})m_1m_2} \qquad (B-12)$$

One can insert $\omega_-{}^2 = \frac{1}{2m_1m_2}[(m_1+m_2)(\Gamma_2+\Gamma_1) - \sqrt{(m_1+m_2)^2(\Gamma_2+\Gamma_1)^2 - 16\Gamma_1\Gamma_2 sin^2(\frac{ka}{2})m_1m_2}$ into dynamic matrix as shown in Equation 9

$$\frac{1}{2m_1m_2}[(m_1-m_2)(\Gamma_2+\Gamma_1) - \sqrt{(m_1+m_2)^2(\Gamma_2+\Gamma_1)^2 - 16\Gamma_1\Gamma_2 sin^2(\frac{ka}{2})m_1m_2}]e_1(k,s)$$
$$+ \frac{1}{\sqrt{m_1}\sqrt{m_2}}(\Gamma_1 + \Gamma_2 exp(-ika))e_2(k,s) = 0 \qquad (B-13)$$

$$\frac{e_2(k,s)}{e_1(k,s)} = \frac{\frac{1}{2m_1m_2}[(m_2-m_1)(\Gamma_2+\Gamma_1) + \sqrt{(m_1+m_2)^2(\Gamma_2+\Gamma_1)^2 - 16\Gamma_1\Gamma_2 sin^2(\frac{ka}{2})m_1m_2}]}{\frac{1}{\sqrt{m_1}\sqrt{m_2}}(\Gamma_1+\Gamma_2 exp(-ika))} \qquad (B-14)$$

$$\frac{e_2(k,s)}{e_1(k,s)}\frac{e_2*(k,s)}{e_1*(k,s)}$$
$$= \frac{(\frac{1}{2m_1m_2}[(m_2-m_1)(\Gamma_2+\Gamma_1) + \sqrt{(m_1+m_2)^2(\Gamma_2+\Gamma_1)^2 - 16\Gamma_1\Gamma_2 sin^2(\frac{ka}{2})m_1m_2}])^2}{\frac{1}{\sqrt{m_1}\sqrt{m_2}}(\Gamma_1+\Gamma_2 exp(-ika))\frac{1}{\sqrt{m_1}\sqrt{m_2}}(\Gamma_1+\Gamma_2 exp(ika))}$$
$$= \frac{(\frac{1}{2m_1m_2}[(m_2-m_1)(\Gamma_2+\Gamma_1) + \sqrt{(m_1+m_2)^2(\Gamma_2+\Gamma_1)^2 - 16\Gamma_1\Gamma_2 sin^2(\frac{ka}{2})m_1m_2}])^2}{\frac{1}{m_1m_2}(\Gamma_1\Gamma_1+\Gamma_2\Gamma_2+2\Gamma_1\Gamma_2 cos(ka))} \qquad (B-15)$$

Set $\eta = \frac{m_1}{m_2}$ *and* $\xi = \frac{\Gamma_1}{\Gamma_2}$

$$\frac{|e_2(k,s)|}{|e_1(k,s)|} = \frac{\left[(1-\eta)(\xi+1) + \sqrt{(\eta+1)^2(1+\xi)^2 - 16\xi sin^2\left(\frac{ka}{2}\right)\eta}\right]}{2\sqrt{\eta}\sqrt{(1+\xi)^2 - 2\xi\big(1-cos(ka)\big)}} \qquad (B-16)$$

One inset $\omega_+{}^2 = \frac{1}{2m_1m_2}[(m_1+m_2)(\Gamma_2+\Gamma_1) + \sqrt{(m_1+m_2)^2(\Gamma_2+\Gamma_1)^2 - 16\Gamma_1\Gamma_2 sin^2(\frac{ka}{2})m_1m_2}]$ into Equation B-9

$$\frac{e_2(k,s)}{e_1(k,s)}\frac{e_2*(k,s)}{e_1*(k,s)}$$

$$= \frac{(\frac{1}{2m_1m_2}[(m_1-m_2)(\Gamma_2+\Gamma_1) + \sqrt{(m_1+m_2)^2(\Gamma_2+\Gamma_1)^2 - 16\Gamma_1\Gamma_2 sin^2(\frac{ka}{2})m_1m_2}])^2}{\frac{1}{\sqrt{m_1}\sqrt{m_2}}(\Gamma_1+\Gamma_2 exp(-ika))\frac{1}{\sqrt{m_1}\sqrt{m_2}}(\Gamma_1+\Gamma_2 exp(ika))}$$

$$= \frac{(\frac{1}{2m_1m_2}[(m_1-m_2)(\Gamma_2+\Gamma_1) + \sqrt{(m_1+m_2)^2(\Gamma_2+\Gamma_1)^2 - 16\Gamma_1\Gamma_2 sin^2(\frac{ka}{2})m_1m_2}])^2}{\frac{1}{m_1m_2}(\Gamma_1\Gamma_1+\Gamma_2\Gamma_2+2\Gamma_1\Gamma_2 cos(ka))} \qquad (B-17)$$

$$\frac{|e_2(k,s)|}{|e_1(k,s)|} = \frac{\frac{1}{2m_1m_2}[(m_1-m_2)(\Gamma_2+\Gamma_1) + \sqrt{(m_1+m_2)^2(\Gamma_2+\Gamma_1)^2 - 16\Gamma_1\Gamma_2 sin^2(\frac{ka}{2})m_1m_2}]}{\sqrt{\frac{1}{m_1m_2}((\Gamma_2+\Gamma_1)^2 - 2\Gamma_2\Gamma_1(1-cos(ka)))}}$$

$$= \frac{(\eta-1)(1+\xi) + \sqrt{(1+\eta)^2(1+\xi)^2 - 16\eta\xi sin^2(\frac{ka}{2})}]}{2\sqrt{\eta}\sqrt{(1+\xi)^2 - 2\xi(1-cos(ka))}} \qquad (B-18)$$